

Sub-1100 nm lasing from post-growth intermixed InAs/GaAs quantum-dot lasers

H.H. Alhashim, M.Z.M. Khan, M.A. Majid, T.K. Ng and B.S. Ooi[✉]

Impurity free vacancy disordering induced highly intermixed InAs/GaAs quantum-dot lasers are reported with high internal quantum efficiency (>89%). The lasers are shown to retain the device characteristics after intermixing and emitting in the important wavelength of ~1070–1190 nm. The non-coated facet Fabry-Pérot post-growth wavelength tuned lasers exhibits high-power (>1.4W) and high-gain (~50 cm⁻¹), suitable for applications in frequency doubled green-yellow-orange laser realisation, gas sensing, metrology etc.

Introduction: Various assessments of the trends in population, urbanisation, energy and resources etc. and their implications call for environmental sustainability. The energy efficient, environmental-friendly semiconductor quantum-dot (Qdot) laser diode has this potential and certainly is one of the sustainability solutions to address these concerns beside the global information system. InAs/GaAs Qdot lasers possess the distinct advantages of reduced threshold current density, temperature sensitivity, filamentation and mirror degradation, thus enabling the realisation of high-power and high-performance devices [1]. Moreover, InAs/GaAs Qdot emission coverage of ~1060–1400 nm has been employed for the development of optoelectronic devices not only for optical communications but also for a plethora of multidisciplinary field applications [2]. In particular, the short wavelength emission of ~1060–1200 nm has recently attracted attention because of the possibility of coherent light generation in the green-yellow-orange wavelength band via frequency doubling, a cost-effective and compact device for potential incorporation in pico-projectors, semiconductor laser based solid state lighting etc. [1, 2]. This short wavelength region was dominated by the highly strained InGaAs/GaAs and InGaAsN/GaAs multiple-quantum well active region laser designs until recently as-grown (AG) InGaAs/GaAs Qdot based lasers emitting at ~1060–1100 nm have been reported with high power, temperature stability and high gain [1, 3]. However, the growth process was assisted by various schemes such as tunnelling [3], monolayers periodic depositions of InGaAs and InAs material for InGaAs Qdot self-assembled growth [1], and the height limiting growth method [2], to achieve these wavelengths, which adds complexity and cost to device design and fabrication process.

In this Letter, by employing a simple and cost-effective impurity free vacancy disordering (IFVD) post-growth bandgap engineering technique [4, 5], we achieved lasing at ~1070–1190 nm from a conventional grown 1300 nm InAs/GaAs Qdot laser while preserving the device characteristics. The highly intermixed broad-area Fabry-Pérot lasers with SiO₂ and Si₃N₄ capped films and annealed at 725°C demonstrated a ground-state (GS) lasing wavelength blue shift of >185 nm (~148 meV) with high output power; thus highlighting the potential of these wavelength tuned devices in pumping solid-state and fibre lasers, substitute of solid-state lasers. In addition, the fields of metrology and gas sensing would also benefit from bandgap tuned Qdot lasers. Qdot laser based gas sensors will enable the detection of H₂O, HBr, HI, HCl molecules, ethanol and water in gasoline etc. for process and environmental control [6]. The low atmospheric absorption window of ~1000–1100 nm will facilitate the deployment of these small-footprint lasers in light detection and ranging systems where currently 1064 nm Nd-YAG lasers dominate [7], besides being a potential light source for free space optical communications.

Experiment: The material was grown by molecular beam epitaxy on (100) oriented n-type S-doped GaAs substrate. The active region consists of eight Qdot stacks with each 40 nm thick layer incorporating InAs Qdot layer covered with InGaAs strain reducing layer and followed by partially p-doped GaAs barrier. The active region was sandwiched between n-type (p-type) Al_{0.4}Ga_{0.6}As lower(upper) cladding layers with 400 nm heavily doped p-type GaAs contact layer. Three samples were cleaved from the laser wafer and on two of them 200 nm-thick SiO₂ and Si₃N₄ dielectric caps were deposited using plasma-enhanced chemical vapour deposition. These samples were then subjected to rapid thermal processing in nitrogen ambient at temperatures of 650 to 725°C in steps of 25°C for 120 s and under As over-pressure. Power

density dependent photoluminescence (PL) measurements at 77 K were performed on these samples, in addition to the third AG sample, to evaluate the degree of bandgap shift. Later, broad area lasers with a 50 μm stripe width were fabricated from the three samples using a standard laser fabrication process (under an identical environment), after removing the capping layer and cleaved into bars of different cavity lengths (0.2–3.0 mm) with as-cleaved facets and tested under pulsed current operation (2.0 μs current pulse width and 2% duty cycle) with thermo-electric cooling and p-side up mounting configuration.

Results and discussion: 77 K PL results at an excitation power density of 2.3 kW/cm² are shown in Fig. 1, corresponding to the SiO₂ and Si₃N₄ capped Qdot samples annealed at 725°C, in addition to the PL spectrum of the AG sample. A significant GS peak blue shift of ~145 nm (~142 meV) is observed between the AG (~1200 nm) and annealed SiO₂ (~1055 nm) capped sample, accompanied by considerable narrowing of the PL linewidth to ~25 nm (~40% of the AG sample, obtained via Gaussian fit). In addition, the GS peak PL and integrated PL intensities showed improvement by ~3.0 and ~1.5 times, respectively, compared with the AG sample. This is attributed to the efficient sinking of Ga by the SiO₂ film and enhanced vacancy diffusion deeper into the sample because of the high compressive strain developed at the SiO₂/GaAs interface during thermal annealing [4, 5]. The GS and ES inter-subband spacing is found to reduce in both the annealed samples with a single emission peak from the SiO₂ capped sample and screening of inefficient ES emission (with a faint short wavelength shoulder at 1030 nm). Alternatively, the Si₃N₄ capped sample at 725°C showed a slower In-Ga inter-diffusion rate and clear two peak emissions at ~1074 (GS) and ~1032 nm (ES), with a GS peak emission blue shift of ~126 nm (~121 meV) compared with the AG sample. These results are consistent with the literature and are attributed to the smaller compressive stress induced at the film/GaAs interface by the SiO₂ compared with the Si₃N₄ capping layer [4]. This is further affirmed by the annealing temperature dependent investigation (inset of Fig 1) which showed an inhibition of vacancy diffusion at <675°C and intermixing effects from ≥675°C. The GS peak PL (integrated PL), in this case, is also found to improve by ~2.0 (~1.5) times the AG sample besides reduction in the GS PL linewidth (~15% reduction compared with the AG sample). Thus, both the dielectric capping at high annealing temperature improved the material optical quality, thus showing the effectiveness of this simple method to tailor the energy states of Qdots for desired applications.

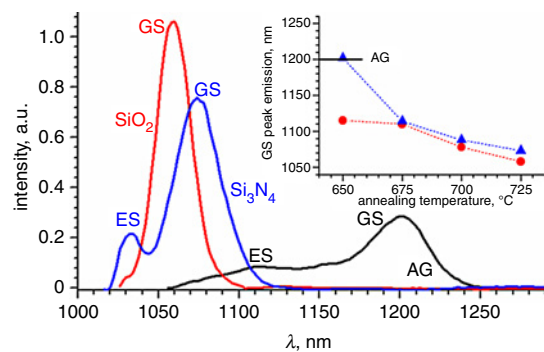


Fig. 1 77 K PL spectra of AG and 725°C annealed SiO₂ and Si₃N₄ capped Qdot laser structure.

Inset: Summary of changes in GS peak emission against annealing temperatures with indicated AG sample value

Fig. 2 depicts the total device (two identical facets) output power-current (*L-I*) characteristics of the annealed (SiO₂ and Si₃N₄ capped) laser diodes at room temperature and at different cavity lengths. The summary of the lasing wavelengths against cavity length is plotted in Fig. 3 besides the AG laser results. A single lasing wavelength of ~1070 nm (~1108 nm) at ES with a total optical power of 0.8 (0.5) W is measured from the SiO₂ (Si₃N₄) capped short cavity [0.25 mm (0.3 mm) for SiO₂ (Si₃N₄)] devices while the long cavity [1.25 mm (3.0 mm) for SiO₂ (Si₃N₄)] broad-area lasers exhibited an output power in excess of 1.5 W (1.4 W) at GS lasing of ~1118 nm (~1190 nm). A slope efficiency of ~0.95 (~0.82) W/A from SiO₂ and ~0.71 (~0.40) W/A from Si₃N₄ annealed short (long) cavity lasers is measured

which corresponds to a differential quantum efficiency (η_d) of $\sim 81\%$ ($\sim 74\%$) and $\sim 64\%$ ($\sim 39\%$). Moreover, no power roll-over in the L - I curves suggests possible achievement of even higher output power values. On the other hand, the AG Qdot laser showed a lasing wavelength of ~ 1300 nm (~ 1240 nm) from the GS (ES) emission, as summarised in Fig. 3 and a slope efficiency of ~ 0.4 (0.6) W/A from 0.2 mm (2.0 mm) cavity lasers. Compared with the AG laser results, annealed lasers exhibited a lasing wavelength blue shift of >180 nm with better slope efficiency (SiO_2 capped lasers were found to be superior to Si_3N_4 capped lasers) and a noted decrease in their lasing bandwidths (not shown).

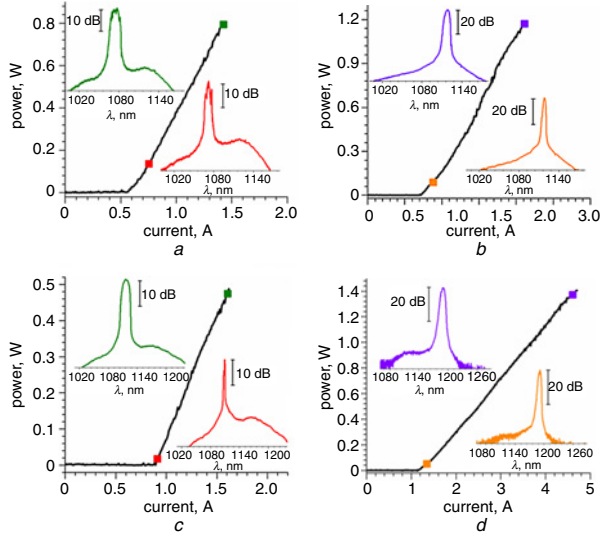


Fig. 2 Room temperature L - I characteristics of $50 \mu\text{m}$ stripe width annealed SiO_2 and Si_3N_4 laser diodes with different cavity lengths

a 0.3 mm-long SiO_2 capped Qdot laser
b 1.25 mm-long SiO_2 capped Qdot laser
c 0.25 mm-long Si_3N_4 capped Qdot laser
d 3.0 mm-long Si_3N_4 capped Qdot laser

Insets: Lasing spectra at respective indicated injection currents

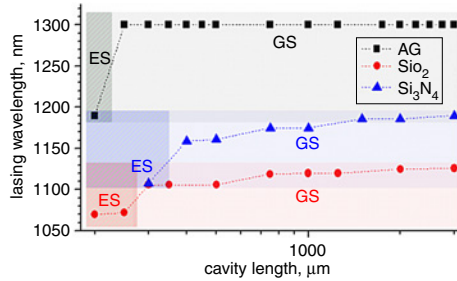


Fig. 3 Cavity length dependent lasing wavelength (just above threshold) from AG, and 725°C annealed SiO_2 and Si_3N_4 capped Qdot lasers at room temperature.

Table 1: Summary of extracted AG and annealed laser performance parameters with error margin of $\pm 5\%$

| Sample | J_0 (A/cm^2) | η_i (%) | α_i (cm^{-1}) | T_0 (K) | Γ_{gsat} (cm^{-1}) |
|-----------------------------|----------------------------------|--------------|---------------------------------|------------|---|
| AG | 330 | 87 | 4.4 | ~ 295 | 53 |
| SiO_2 cap | 604 | 93 | 5.2 | ~ 65 | 50 |
| Si_3N_4 cap | 634 | 89 | 6.3 | ~ 55 | 39 |

We further compared the lasers' performance by extracting the internal quantum efficiency (η_i), internal loss (α_i), transparency current density (J_0), characteristics temperature (T_0) and the GS saturated modal gain (Γ_{gsat}). The results are summarised in Table 1. An increase in J_0 is observed in the annealed devices compared with the AG device which is attributed to the reduction in the optical confinement factor as a result of Qdot size reduction, and to the weakly localised Qdot layers because of reduced conduction band offsets as a result of annealing (blue shift of lasing wavelength) [8]. In fact, T_0 is also found to reduce possibly because of the latter effect, thus promoting the thermal injection of carriers out of the Qdots. Alternatively, an

improvement in η_i from 87% (AG) to 93% (SiO_2) and 89% (Si_3N_4) is derived with a small increase in α_i value being observed. This is ascribed to the possible annealing of the defects at high temperatures which might be present near the Qdot-barrier interface owing to the low temperature growth process, in addition to the high stress field around the Qdots [5]. The small increase in α_i might be a result of minor alteration in the scattering loss of photons because of localised variation of the refractive index at the Qdot-barrier interface and the doping profile during annealing. The cumulative effect of these parameters resulted in a minor decrease (0.5 cm^{-1} per layer) in the GS saturated modal gain of the SiO_2 capped Qdot laser whereas the Si_3N_4 capped laser showed a decrease of 1.75 cm^{-1} per layer. In general, all these parameters indicate a comparable performance from IFVD tuned Qdot lasers, able to lase in the ~ 1070 – 1190 nm range with almost preserved active region optical quality and inhomogeneity. We believe that an optimised design of the laser active region with enough conduction band offset would further improve the annealed laser performance parameters.

Conclusion: A simple cost-effect post-growth bandgap engineering method is demonstrated on InAs/GaAs Qdot laser with ~ 185 nm blue shifted Qdot transition states and lasing at ~ 1070 – 1190 nm. The devices are shown to maintain their performance characteristics. Such high-power devices pave a way for the potential achievement of visible light via the frequency doubling technique besides other cross-disciplinary field applications. The current demonstration also paves a way for possible realisation of multiple wavelength application from a single dedicated wavelength (1300 nm) InAs/GaAs Qdot epitaxial wafer.

Acknowledgment: This work was supported by a KAUST competitive research grant (CRG-1-2012-OOI-010) and baseline funding.

This is an open access article published by the IET under the Creative Commons Attribution License (<http://creativecommons.org/licenses/by/3.0/>) This is an open access article published by the IET under the Creative Commons Attribution License (<http://creativecommons.org/licenses/by/3.0/>)

Submitted: 24 May 2015

doi: 10.1049/el.2015.1803

One or more of the Figures in this Letter are available in colour online.

H.H. Alhashim, M.Z.M. Khan, M.A. Majid, T.K. Ng and B.S. Ooi (Photonics Laboratory, Computer, Electrical, and Mathematical Sciences and Engineering (CEMSE) Division, King Abdullah University of Science and Technology (KAUST), Thuwal 23955-6900, Saudi Arabia)

✉ E-mail: boon.ooi@kaust.edu.sa

References

- Pavelescu, E., Gilfert, C., Weinmann, P., Dănilă, M., Dinescu, A., Jacob, M., Kamp, M., and Reithmaier, J.: '1100 nm InGaAs/(Al) GaAs quantum dot lasers for high-power applications', *J. Phys. D, Appl. Phys.*, 2011, **44**, (14), p. 145104
- Watanabe, K., Akiyama, T., Yokoyama, Y., Takemasa, K., Nishi, K., Tanaka, Y., Sugawara, M., and Arakawa, Y.: 'Growth of high-density 1.06- μm InGaAs/GaAs quantum dots for high gain lasers by molecular beam epitaxy', *J. Cryst. Growth*, 2013, **378**, pp. 627–630
- Pavelescu, E.-M., Gilfert, C., Reithmaier, J.P., Martin-Minguez, A., and Esquivias, I.: 'High-power tunnel-injection 1060-nm InGaAs-(Al) GaAs quantum-dot lasers', *IEEE Photonics Technol. Lett.*, 2009, **21**, (14), pp. 999–1001
- Lever, P., Tan, H.H., and Jagadish, C.: 'Impurity free vacancy disordering of InGaAs quantum dots', *J. Appl. Phys.*, 2004, **96**, (12), pp. 7544–7548
- Djie, H.S., Wang, Y., Ooi, B.S., Wang, D.-N., Hwang, J., Dang, G.T., and Chang, W.H.: 'Defect annealing of InAs-InAlGaAs quantum-dash-in-asymmetric-well laser', *IEEE Photonics Technol. Lett.*, 2006, **18**, (21–24), pp. 2329–2331
- Zeller, W., Nahle, L., Fuchs, P., Gerschuetz, F., Hildebrandt, L., and Koeth, J.: 'DFB lasers between 760 nm and 16 μm for sensing applications', *Sensors*, 2010, **10**, (4), pp. 2492–2510
- Hu, Y., Starnes, K., Vaughan, M., Pelon, J., Weimer, C., Wu, D., Cisewski, M., Sun, W., Yang, P., and Lin, B.: 'Sea surface wind speed estimation from space-based lidar measurements', *Atmos. Chem. Phys.*, 2008, **8**, (13), pp. 3593–3601
- Nikitina, E., Zhukov, A., Vasil'ev, A., Semenova, E., Gladyshev, A., Kryzhanovskaya, N., Maksimov, M., Shernyakov, Y.M., Ustinov, V., and Ledentsov, N.: 'Lasing wavelength of quantum dot heterostructures controlled within the 1.3–0.85 μm range by means of high-temperature annealing', *Tech. Phys. Lett.*, 2004, **30**, (8), pp. 644–646